

# A multispectrum fitting procedure to deduce molecular line parameters: Application to the 3-0 band of $^{12}\text{C}^{16}\text{O}$

D. Jacquemart<sup>1</sup>, J.-Y. Mandin<sup>1</sup>, V. Dana<sup>1,a</sup>, N. Picqué<sup>2</sup>, and G. Guelachvili<sup>2</sup>

<sup>1</sup> Laboratoire de Physique Moléculaire et Applications, CNRS et Université Pierre et Marie Curie, case 76, tour 13, 4 place Jussieu, 75252 Paris Cedex 05, France

<sup>2</sup> Laboratoire de Photophysique Moléculaire, CNRS et Université Paris-Sud, bâtiment 350, 91405 Orsay Cedex, France

Received 21 September 2000 and Received in final form 15 January 2001

**Abstract.** To deduce accurate infrared molecular line parameters (positions at zero pressure, pressure-shifting and pressure-broadening coefficients, collisional narrowing coefficients, and intensities) from rovibrational spectra, an automatic method based upon a multispectrum fitting procedure has been set up, able to treat simultaneously several laboratory Fourier transform spectra. A validation of this method, using absorption spectra of the 3-0 vibrational band of CO around  $6\,350\text{ cm}^{-1}$ , already used to measure line intensities and self-broadening coefficients, is presented, and the advantages of the method are pointed out. The self-collisional narrowing of CO was observed and determined for the first time in Fourier transform spectra:  $\beta_0 = 0.028 \pm 0.004\text{ cm}^{-1}\text{ atm}^{-1}$  at about 296 K.

**PACS.** 33.20.Ea Infrared spectra – 33.70.Fd Absolute and relative line and band intensities – 33.70.Jg Line and band widths, shapes, and shifts

## 1 Introduction

The simultaneous treatment of several experimental spectra, in order to derive unknown parameters through a non-linear least-squares method, is frequently used in atmospheric spectroscopy [1], typically when one wants to obtain the vertical distribution of minor constituents. In this case, molecular line parameters, as positions, pressure-shifts, intensities, or collisional widths, are well known, whereas absorbing gas amounts at different altitudes are looked for. Our aim is the reverse: to profit by the advantages of the simultaneous treatment of several laboratory spectra, in order to deduce line parameters knowing the experimental conditions. A few teams [2, 3] have developed such a multispectrum fitting procedure (see Appendix A, Sect. A.5)<sup>1</sup> applied to laboratory spectra. Many advantages were found in this technique and were already pointed out [2,3]: possibility to fit spectra obtained at different resolutions or recorded with different spectrometers, ability to obtain parameters that cannot be determined from a single spectrum, and improvement in the statistical uncertainties. A multispectrum procedure was set up in this work. Our main goal was to have at our disposal a tool more efficient than the usual spectrum-by-spectrum method (A.5), and able to deduce some parameters particularly difficult to determine, as collisional narrowing coefficients, data that will be more and more

requested for precise atmospheric applications in a near future. Also, cross comparisons of the results obtained from relatively complicated codes could then be scheduled between different teams. During the validation of the procedure, we confirmed the previously quoted advantages and showed off new advantages. This paper was also the opportunity to enlight these advantages in a way different from this of other authors.

Our multispectrum procedure is an extension of a previous automatic method [4,5] used to treat Fourier transform spectra: the adjustable or fixed parameters are, first, those of the involved rovibrational lines (positions at zero pressure, pressure-shifting and pressure-broadening coefficients, collisional narrowing coefficients, and intensities), and, second, some parameters dependent on the spectrum (effective iris radius needed to calculate the “*étendue*”, phase error if any, and continuous background). Section 2 will be devoted to the description of the procedure. We have validated this method with Fourier transform absorption spectra of the 3-0 vibrational band of CO around  $6\,350\text{ cm}^{-1}$  which were already used by Picqué *et al.* [6] to measure line intensities and self-broadening coefficients. In Section 3, the results of this validation will be presented and discussed as typical examples able to show up the advantages of the method. Furthermore, one will see how the multispectrum procedure allowed the determination of the CO self-collisional narrowing coefficient, whereas this determination was not possible with the usual spectrum-by-spectrum method, mainly because of the weakness of this effect observed for the first time in Fourier transform spectra of the CO molecule.

<sup>a</sup> e-mail: vdana@ccr.jussieu.fr

<sup>1</sup> The last section of the Appendix is a glossary (hereafter referred to as A.5) of the main terms used for the sake of this paper.

## 2 Description of the multispectrum procedure

The principle of the non-linear least-squares method is well known and one will recall only what is necessary (see, *e.g.* [7]): an observed data vector  $\tau_{\text{exp}}$  ( $q$ -dimensional) is given and the response function vector  $\tau_{\text{calc}}(\theta)$  is calculated with respect to the free parameters vector  $\theta$  ( $p$ -dimensional); the best values of the free parameters are then obtained minimizing the length of the vectorial difference  $\tau_{\text{calc}}(\theta) - \tau_{\text{exp}}$ , *i.e.* minimizing the sum of squares of the observed – calculated residuals. In absorption spectroscopy, the elements of  $\tau$  are the sampled transmission, *i.e.* the ratio between the transmitted and incident intensities of the beam. The vector  $\tau_{\text{exp}}$  represents a fixed point  $M$  in a  $q$ -dimensional space, and  $\tau_{\text{calc}}(\theta)$  is the parametric representation of a  $p$ -dimensional sub-ensemble  $\mathcal{E}_p$  of this space. The best parameters vector corresponds to the point of  $\mathcal{E}_p$  closest to  $M$ . When  $p$  equals  $q$ ,  $\mathcal{E}_p$  has  $q$  dimensions and since it should contain  $M$  (otherwise, the theoretical model used to calculate  $\tau_{\text{calc}}(\theta)$  is wrong), there exists an exact solution  $\theta_0$  corresponding to  $\tau_{\text{calc}}(\theta_0) \equiv \tau_{\text{exp}}$ . Conversely, the principle of the multispectrum method is to improve the data reduction increasing  $q$  (more spectra, therefore more data) and decreasing  $p$  (less parameters). For both multispectrum and usual spectrum-by-spectrum methods, the whole vectors  $\tau_{\text{exp}}$  and  $\tau_{\text{calc}}$  are obtained concatenating the corresponding vectors associated with the  $N$  studied spectra. In the spectrum-by-spectrum method, the elements of  $\tau_{\text{exp}}$  and  $\tau_{\text{calc}}$  corresponding to different spectra are decoupled, and the method involves  $N \times p$  independent line parameters (without counting the parameters related to the spectra in order to simplify the discussion, the dimension of  $\theta$  is then  $N \times p$ , if  $p$  line parameters are needed per spectrum). This is equivalent to treat separately each spectrum as done in practice. On the contrary, the multispectrum method links the elements corresponding to different spectra, through only  $p$  independent line parameters in the most general case (the dimension of  $\theta$  is now  $p$ ). Intermediate cases can also be imagined where only some of the  $N \times p$  line parameters link the elements belonging to some selected spectra (the dimension of  $\theta$  remains smaller than  $N \times p$  but is greater than  $p$ ). We have used such a possibility in this work.

To treat molecular spectra sometimes very crowded, a method was set up some years ago [4,5], based upon a Gauss-Newton like algorithm published by Ralston and Jennrich [7]. This derivative-free algorithm (called DUD [7], for “Doesn’t Use Derivatives”) was found quick and efficient to converge even in somewhat complicated conditions frequently encountered in molecular spectra, such as strong line overlappings. This method was automatized (A.5), that is to say, the numerous lines present in a spectrum can be treated sequentially without intervention of the operator. In this method, that we have called the spectrum-by-spectrum method, one set of best line parameters is retrieved for each spectrum, and final parameter values are obtained performing some averages at the end of an iterative manual process, often time consuming since the treatment of typically at least five spectra is usual in molecular spectroscopy. We have extended this method in

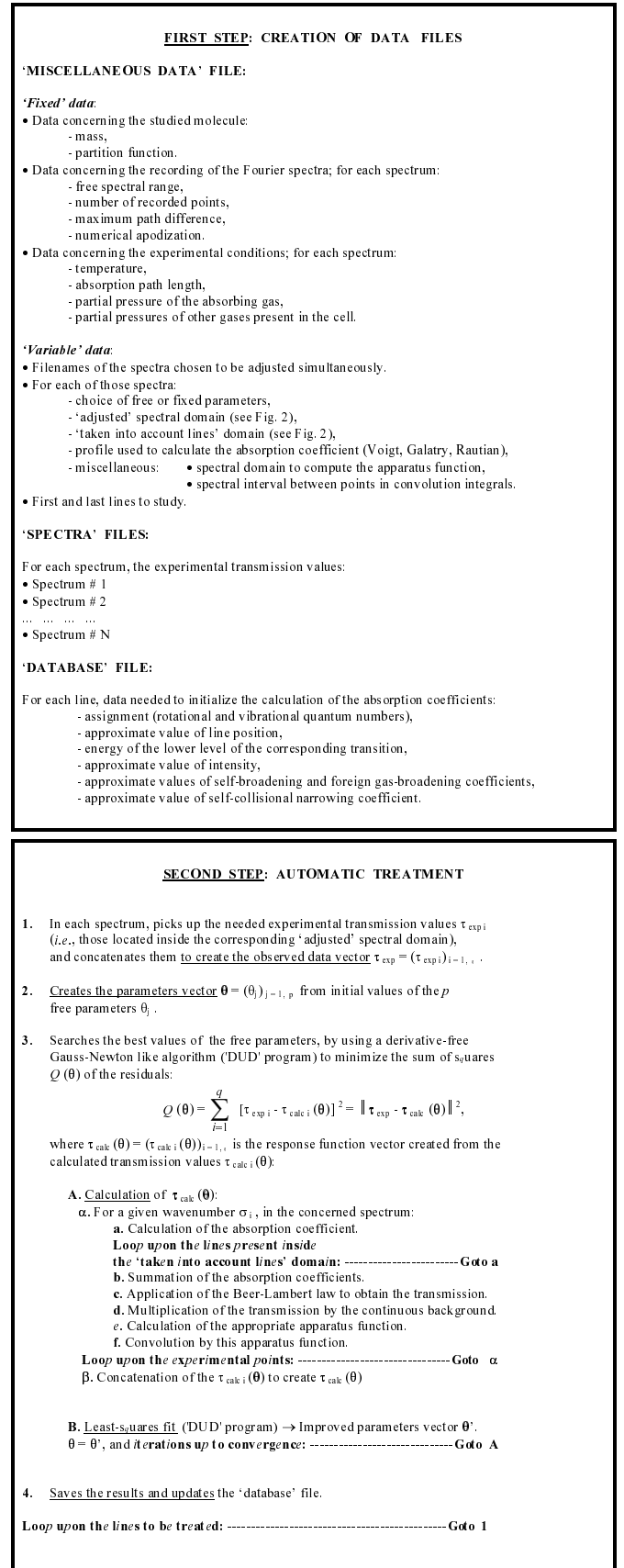


**Fig. 1.** Simplified flow diagram of the automatic multispectrum fitting procedure.

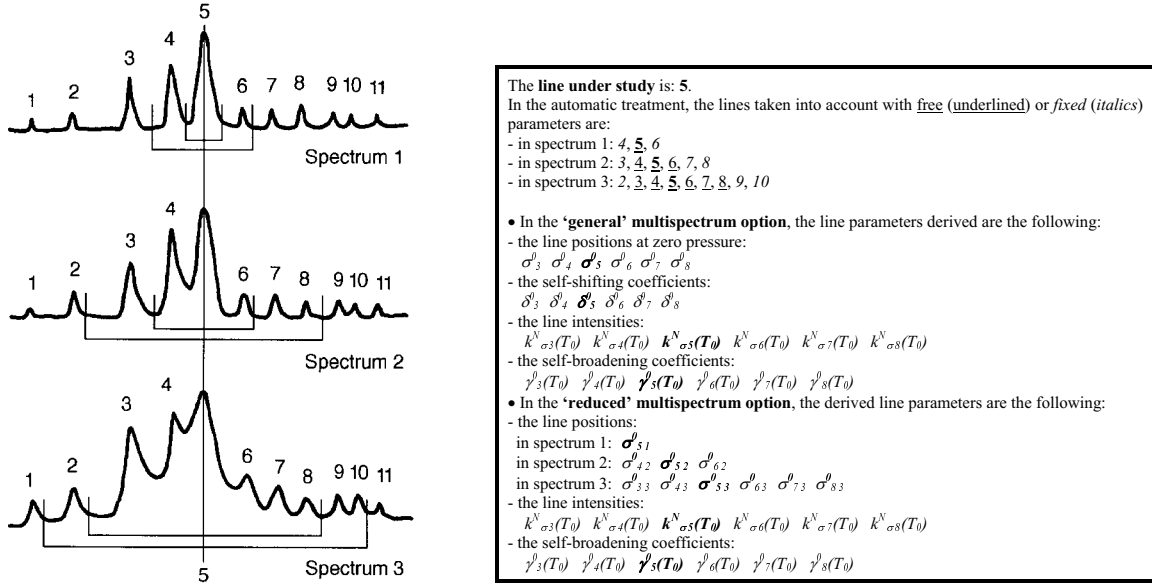


**Fig. 2.** Schematic plot showing the “adjusted” spectral domains and the “taken into account lines” spectral domains, which can be chosen independently for each spectrum according to the experimental conditions. These domains are symmetric around the line under study: the narrowest is the “adjusted” spectral domain, and the largest is the “taken into account lines” spectral domain. An example of utilization of the method, associated with the domains chosen on the plot, is detailed on the right of the plot.

order to treat simultaneously several spectra. Then, the line parameters can be determined at once, without the necessity to perform averages: this is the main advantage of the multispectrum method.

The Appendix, referring to appropriate papers [8–16], recalls the equations needed to calculate the transmission (Eqs. (3–6)) that modelizes the experimental transmission, and a simplified flow diagram is given in Figure 1. The notations can seem rather complicated, and indeed, if the principle of the least-squares method is very simple, its encoding in the case of a multispectrum treatment becomes complicated. For example, it is worth noticing that, in the general case, the calculated transmission function (one speaks about the transmission *function*, not about the *values* of the transmission), that we have noted  $\tau_{\text{calc } i}$  in Figure 1, depends upon the considered experimental point  $i$ , because the absorption coefficient and the apparatus function can both be represented by different functions according to the spectrum from which the experimental point  $i$  belongs. In Figure 2, three spectra have been schematically drawn in order to illustrate the different spectral domains (A.5) used in the procedure, which can be runned automatically or manually (A.5). In the automatic version, the lines are treated sequentially (see Fig. 1). For each spectrum, the “adjusted” spectral domain (A.5) delimits the spectral region where the experimental transmission will be adjusted. To calculate the transmission in these regions, one sums over the absorption coefficients of all the lines whose center is located inside the “taken into account lines” domain of the corresponding spectrum. In each spectrum, those lines whose center is located inside the “adjusted” spectral domain have free parameters, and those located inside the “taken

into account lines” domain (A.5), but outside the “adjusted” spectral domain, have fixed parameters (approximate initial values, or values taken in a database, or becoming from a previous run). For a better versatility, two options were coded: in the “general” multispectrum option (A.5), each free line parameter is constrained to the same value in all the spectra, and in a “reduced” multispectrum option (A.5), the line positions are let free independently in each spectrum, but consequently the line pressure-shifts cannot be adjusted (the interest of this last version will be discussed in Section 3 in the case of difficulties in the calibration of the wavenumber scales). Figure 2 indicates which parameters are free or fixed in these two cases for the plotted example: these examples of utilization of the procedure correspond to the most general capabilities we have coded at the present time, but in most cases, we have checked that the parameters obtained for the studied line are not changed if one chooses the same values for the “adjusted” and the “taken into account lines” domains. Finally, in the manual version, when treating a peculiar line, it is possible to decide which parameter will be constrained or let free for the lines taken into account, and it is also possible to add some lines if necessary.

### 3 Validation of the multispectrum procedure and advantages of this method: application to the 3-0 band of the $^{12}\text{C}^{16}\text{O}$ molecule

#### 3.1 Validation of the multispectrum procedure

To validate the multispectrum fitting procedure, we used several Fourier transform spectra analyzed in a previous

**Table 1.** Experimental conditions and characteristics of the Fourier transform absorption spectra of the 3-0 band of  $^{12}\text{C}^{16}\text{O}$ .

Maximum path difference	81 cm		
Unapodized resolution limit (FWHM)	$6 \times 10^{-3} \text{ cm}^{-1}$		
Effective iris radius	between 2.92 and 3.44 mm		
	according to the spectrum		
Collimator focal length	2000 mm		
Peak-to-peak signal-to-noise ratio	$\approx 1000$		
Commercial sample	Natural CO: 98.65 % of $^{12}\text{C}^{16}\text{O}$		
	Stated purity: 99.997%		
Spectrum #	Total pressure <sup>a</sup> (Torr) <sup>b</sup>	Absorption path <sup>c</sup> (m)	Temperature <sup>d</sup> (K)
1	4.40	32.18	296.65
2	6.50	32.18	297.65
3	4.40	32.18	296.65
4	40.0	16.18	296.85
5	80.0	16.18	296.45
6	300	4.18	295.95
7	761	4.18	295.85

<sup>a</sup>  $\pm 0.5\%$ . <sup>b</sup> 1 torr = 1.333 hPa. <sup>c</sup>  $\pm 1 \text{ cm}$ . <sup>d</sup>  $\pm 1 \text{ K}$ .

work to measure intensities (Eq. (7)) and self-broadening coefficients (Eqs. (14, 15)) of lines in the 3-0 band of  $^{12}\text{C}^{16}\text{O}$  [6]. These spectra have been chosen, first because they have a very good signal-to-noise ratio, and second because the experimental conditions (pressures and absorption path lengths) had been carefully selected to allow an accurate determination both of line intensities and collisional widths (see Tab. 1). Then, these spectra of a simple molecule were a typical example of usage of the spectrum-by-spectrum procedure, interesting to treat comparatively with the multispectrum procedure.

To perform significant comparisons, the two procedures had to be used in conditions as close as possible. Therefore, when running our multispectrum code, we fixed the same values as in [6] for the “adjusted” spectral domain of each spectrum, as also for the effective iris radius and phase errors, and other miscellaneous data used in the computations (see Fig. 1). In the same way, the absorption coefficient was modeled by a Voigt profile (Eqs. (6, 8–10)) as in [6]. An exponent  $m = 0.69$ , found in the HITRAN database [17], was used to take into account the temperature dependence of the self-broadening coefficients (strictly speaking, the value of [17] concerns the air-broadening coefficients of CO lines, but this should have negligible consequences since our spectra have all been recorded under very close temperatures). The temperature dependence of the self-shifting coefficients was neglected, no data being available (this effect should be totally negligible taking into account the experimental uncertainty in the measurement of line shifts). As far as the line intensities are concerned, the energy of the lower levels of the transitions were found in HITRAN [17], and the same partition function value as in [6] was chosen, *i.e.*  $Z(296 \text{ K}) = 107.43$  calculated from the polynomial expansion published by Gamache [18, 19]. The results finally obtained are listed in Tables 2 and 3, together with those of [6] obtained from the spectrum-by-spectrum

method. One can see that these results are very close to each other, showing the coherence of the two methods and of the obtained results. The dispersion of the ratio  $\rho$  between the two types of results ( $\langle \rho \rangle = \text{MSF1} / [6]$  in Tabs. 2 and 3) gives an idea of the whole statistical uncertainty:  $\langle \rho \rangle = 0.9990 \pm 0.0046$  for the line intensities, and  $\langle \rho \rangle = 0.9982 \pm 0.0054$  for the self-broadening coefficients.

### 3.2 Improvements of the line parameters measured in the 3-0 band of $^{12}\text{C}^{16}\text{O}$ owing to the multispectrum method

#### 3.2.1 Treatment of the collisional narrowing observed in the 3-0 band of $^{12}\text{C}^{16}\text{O}$

The multispectrum procedure applied to the CO spectra allowed some slight improvements that we will detail below.

At first, average values of effective iris radius and phase errors could easily be determined for each spectrum. These values were very close to those found in [6], but more significant than in [6]. So, for the sake of coherence, in the final run of the procedure we fixed the values of effective iris radius and phase errors to their average values.

Furthermore, as in [6], we noted weak anomalous “W” signatures (maximum 3% peak-to-peak) in the residuals of the three medium pressure spectra 4-6 (see Tab. 1): these signatures are due to the well known collisional narrowing, or Dicke-Galatry effect [12, 13], which was also observed in diode laser spectra of the 3-0 band of CO recorded by Henningsen *et al.* [20]. In the present work, this effect could be observed for the first time on CO Fourier transform spectra: Figure 3 shows the P6 line adjusted simultaneously in the seven spectra using Voigt profile. We modeled this effect by testing other profiles [14, 15], as the Galatry profile valid in the case of soft collisions, and the Rautian profile [16] valid for hard collisions. Strictly

**Table 2.** Line intensities in the 3-0 band of  $^{12}\text{C}^{16}\text{O}^{\text{a}}$ .

Line	[6]	%	MSF1	%	MSF1/[6]	MSF2	%	$x$ %
P 20	1.29e-24	0.45	1.28e-24	0.58	0.992	1.29e-24	0.49	1.06
P 19	1.81e-24	0.98	1.82e-24	0.38	1.006	1.82e-24	0.35	-0.28
P 18	2.46e-24	0.61	2.46e-24	0.30	1.000	2.47e-24	0.20	0.25
P 17	3.31e-24	0.33	3.30e-24	0.27	0.997	3.31e-24	0.17	-0.20
P 16	4.28e-24	0.37	4.31e-24	0.25	1.007	4.32e-24	0.15	-0.11
P 15	5.49e-24	0.20	5.50e-24	0.23	1.002	5.51e-24	0.13	0.00
P 14	6.90e-24	0.37	6.86e-24	0.23	0.994	6.88e-24	0.12	-0.07
P 13	8.39e-24	0.57	8.39e-24	0.24	1.000	8.43e-24	0.11	-0.59
P 12	9.96e-24	0.45	9.96e-24	0.21	1.000	9.99e-24	0.11	-0.19
P 11	1.16e-23	0.16	1.15e-23	0.21	0.991	1.16e-23	0.11	-0.30
P 10	1.31e-23	0.57	1.30e-23	0.24	0.992	1.31e-23	0.10	-0.32
P 9	1.43e-23	0.49	1.43e-23	0.20	1.000	1.43e-23	0.10	0.22
P 8	1.52e-23	0.45	1.52e-23	0.29	1.000	1.53e-23	0.10	-0.34
P 7	1.57e-23	0.45	1.56e-23	0.19	0.994	1.57e-23	0.10	-0.14
P 6	1.54e-23	0.45	1.55e-23	0.21	1.006	1.55e-23	0.12	-0.06
P 5	1.46e-23	0.41	1.46e-23	0.23	1.000	1.46e-23	0.10	0.12
P 4	1.30e-23	0.41	1.30e-23	0.21	1.000	1.30e-23	0.10	0.00
P 3	1.06e-23	0.33	1.06e-23	0.23	1.000	1.06e-23	0.10	0.35
P 2	7.54e-24	0.53	7.58e-24	0.24	1.005	7.58e-24	0.15	0.17
P 1	3.99e-24	0.37	3.99e-24	0.26	1.000	3.98e-24	0.17	0.25
R 0	4.19e-24	0.53	4.16e-24	0.27	0.993	4.17e-24	0.16	-0.04
R 1	8.27e-24	0.49	8.26e-24	0.23	0.999	8.28e-24	0.12	0.12
R 2	1.21e-23	0.49	1.21e-23	0.22	1.000	1.21e-23	0.10	0.24
R 3	1.54e-23	0.37	1.55e-23	0.20	1.006	1.55e-23	0.10	-0.08
R 4	1.81e-23	0.37	1.82e-23	0.21	1.006	1.82e-23	0.10	0.03
R 5	2.02e-23	0.20	2.01e-23	0.19	0.995	2.01e-23	0.10	0.28
R 6	2.13e-23	0.37	2.13e-23	0.18	1.000	2.13e-23	0.09	-0.01
R 7	2.16e-23	0.24	2.16e-23	0.19	1.000	2.16e-23	0.09	0.16
R 8	2.13e-23	0.45	2.12e-23	0.19	0.995	2.12e-23	0.09	0.19
R 9	2.02e-23	0.24	2.01e-23	0.19	0.995	2.02e-23	0.09	0.08
R 10	1.87e-23	0.33	1.86e-23	0.19	0.995	1.87e-23	0.09	-0.05
R 11	1.68e-23	0.24	1.68e-23	0.20	1.000	1.68e-23	0.10	0.15
R 12	1.47e-23	0.29	1.47e-23	0.24	1.000	1.48e-23	0.10	-0.24
R 13	1.25e-23	0.33	1.26e-23	0.23	1.008	1.27e-23	0.11	-0.45
R 14	1.06e-23	0.24	1.05e-23	0.22	0.991	1.06e-23	0.11	-0.29
R 15	8.67e-24	0.29	8.61e-24	0.24	0.993	8.65e-24	0.13	-0.16
R 16	6.90e-24	0.29	6.89e-24	0.22	0.999	6.92e-24	0.13	-0.31
R 17	5.36e-24	0.20	5.36e-24	0.26	1.000	5.38e-24	0.15	0.24
R 18	4.11e-24	0.61	4.08e-24	0.29	0.993	4.10e-24	0.20	0.56
R 19	3.07e-24	0.49	3.07e-24	0.31	1.000	3.08e-24	0.21	0.23
R 20	2.26e-24	0.45	2.27e-24	0.27	1.004	2.27e-24	0.26	-0.33

<sup>a</sup> Caption of the column headings, from left to right:

- Line: rotational assignment.
- [6]: line intensities in  $\text{cm molecule}^{-1}$  for pure  $^{12}\text{C}^{16}\text{O}$  at 296 K. These values, taken in [6], are average values obtained from six spectra (the spectrum number 4 was omitted in [6] because of the collisional narrowing).
- %: statistical uncertainty, in percentage, of the previous values, equal to the experimental dispersion quoted in [6] divided by  $\sqrt{6}$ .
- MSF1: our line intensities, obtained by the multispectrum fitting procedure using the same six spectra as for the results of column [6]. Three significant digits have been reported since, as stated in [6], the whole accuracy is 6% in line intensities.
- %: statistical uncertainty of our MSF1 results, equal to the 68% confidence interval, *i.e.* one standard deviation, in percentage. (Note that the statistical uncertainties obtained for the P19 and P20 lines are larger than for the other lines: this is because of the presence of very weak lines, due to traces of  $\text{CO}_2$  inside the evacuated tank of the interferometer.)
- MSF2: best values of line intensities, obtained by the multispectrum fitting procedure from the seven spectra, taking into account the collisional narrowing.
- %: statistical uncertainty of our MSF2 results, equal to the 68% confidence interval, *i.e.* one standard deviation, in percentage.
- $x$  %: in percentage, ratio  $(\text{calc} - \text{MSF2})/\text{MSF2}$ , the calculated intensity being obtained from equation (1) of this paper and equation (1) of [6].

**Table 3.** Self-broadening coefficients in the 3-0 band of  $^{12}\text{C}^{16}\text{O}^{\text{a}}$ .

Line	[6]	%	MSF1	%	MSF1/[6]	MSF2	%	$x$ %
P 20	54.4	0.23	54.5	0.91	1.002	54.9	0.77	0.84
P 19	57.4	0.46	56.5	0.57	0.984	56.6	0.55	-0.34
P 18	57.3	1.10	57.2	0.46	0.998	57.8	0.31	-0.55
P 17	58.8	0.75	58.2	0.40	0.990	58.7	0.26	-0.24
P 16	59.2	0.40	59.3	0.37	1.002	59.7	0.23	-0.18
P 15	60.3	0.17	60.4	0.37	1.002	60.9	0.20	-0.53
P 14	61.4	0.23	61.4	0.35	1.000	61.8	0.18	-0.48
P 13	62.8	0.87	62.3	0.35	0.992	62.6	0.17	-0.35
P 12	63.3	0.29	63.2	0.31	0.998	63.5	0.16	-0.43
P 11	64.1	0.12	64.2	0.31	1.002	64.5	0.23	-0.66
P 10	65.0	0.58	65.0	0.38	1.000	65.2	0.18	-0.37
P 9	65.7	0.58	66.0	0.30	1.005	66.2	0.15	-0.39
P 8	67.1	0.81	67.1	0.54	1.000	67.3	0.16	-0.32
P 7	68.2	0.35	68.3	0.28	1.001	68.4	0.15	0.10
P 6	69.8	0.52	70.0	0.32	1.003	70.2	0.20	-0.02
P 5	72.1	0.52	72.5	0.31	1.006	72.6	0.16	-0.37
P 4	74.7	0.23	75.1	0.37	1.005	75.3	0.15	-0.37
P 3	78.1	0.64	78.2	0.32	1.001	78.4	0.15	-0.02
P 2	81.9	0.75	82.2	0.32	1.004	82.3	0.21	0.30
P 1	87.5	0.29	87.7	0.34	1.002	87.9	0.24	-0.26
R 0	88.2	1.33	87.0	0.39	0.986	87.4	0.22	0.32
R 1	82.2	0.81	82.3	0.31	1.001	82.5	0.17	0.06
R 2	78.1	0.81	78.3	0.30	1.003	78.5	0.15	-0.15
R 3	74.8	0.75	75.0	0.28	1.003	75.1	0.15	-0.11
R 4	71.9	0.58	72.1	0.30	1.003	72.2	0.15	0.18
R 5	70.3	0.58	69.8	0.29	0.993	70.0	0.15	0.26
R 6	68.3	0.52	68.1	0.28	0.997	68.0	0.15	0.69
R 7	66.8	0.52	66.5	0.29	0.996	66.6	0.15	0.73
R 8	65.5	0.64	65.4	0.29	0.998	65.5	0.15	0.67
R 9	64.7	0.52	64.4	0.30	0.995	64.6	0.15	0.56
R 10	64.2	0.46	63.4	0.30	0.988	63.6	0.15	0.75
R 11	63.2	0.52	62.6	0.32	0.991	62.8	0.16	0.68
R 12	61.7	0.58	61.7	0.41	1.000	61.9	0.18	0.78
R 13	61.0	0.46	60.9	0.35	0.998	61.2	0.18	0.50
R 14	59.9	0.40	59.8	0.34	0.998	60.2	0.17	0.63
R 15	59.1	0.35	58.6	0.35	0.992	59.0	0.20	1.01
R 16	58.0	0.52	57.7	0.33	0.995	58.2	0.21	0.61
R 17	56.8	0.35	56.3	0.39	0.991	56.8	0.33	1.21
R 18	55.3	0.35	55.2	0.44	0.998	55.7	0.32	1.27
R 19	54.7	0.92	54.5	0.49	0.996	55.0	0.34	0.65
R 20	53.8	0.81	54.1	0.43	1.006	54.5	0.41	-0.18

<sup>a</sup> Caption of the column headings, from left to right:

- Line: rotational assignment.
- [6]: self-broadening coefficients, in  $10^{-3} \text{ cm}^{-1} \text{ atm}^{-1}$  at 296 K. These values, taken in [6], are average values obtained from three spectra.
- %: statistical uncertainty, in percentage, of the previous values, equal to the experimental dispersion quoted in [6] divided by  $\sqrt{3}$ .
- MSF1: our self-broadening coefficients, obtained by the multispectrum fitting procedure using the same three spectra as for the results of column [6]. Three significant digits have been reported since, as stated in [6], the whole accuracy is 4% in self-broadening coefficients.
- %: statistical uncertainty of our MSF1 results, equal to the 68% confidence interval, *i.e.* one standard deviation, in percentage.
- MSF2: best values of self-broadening coefficients, obtained by the multispectrum fitting procedure from the seven spectra, taking into account the collisional narrowing.
- %: statistical uncertainty of our MSF2 results, equal to the 68% confidence interval, *i.e.* one standard deviation, in percentage.
- $x$  %: in percentage, ratio  $(\text{calc} - \text{MSF2})/\text{MSF2}$ , the calculated self-broadening coefficient being obtained from equation (2).

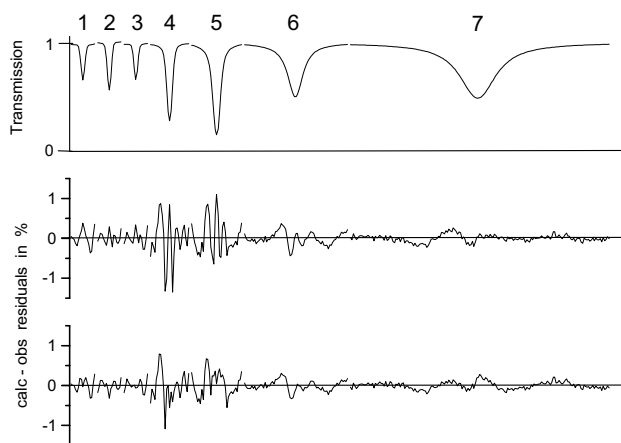


**Fig. 3.** Multispectrum adjustment of the 3-0  $P_6$  line of  $^{12}\text{C}^{16}\text{O}$  at  $6325.799\text{ cm}^{-1}$ , using only Voigt profiles (upper residuals) and introducing Rautian profiles to take into account the self-collisional narrowing (lower residuals). The plots of the lines and of their residuals have been placed side by side, in the order of the spectrum numbers (see Tab. 1) from left to right (such a disposition is more legible than a superimposition of the numerous plots corresponding to different spectra). The wavenumber scales are the same for all the plots: the “adjusted” spectral domains being  $0.2\text{ cm}^{-1}$ ,  $0.3\text{ cm}^{-1}$ ,  $0.4\text{ cm}^{-1}$ ,  $0.6\text{ cm}^{-1}$ , and  $2\text{ cm}^{-1}$  for respectively spectra 1–3, 4, 5, 6, and 7. The upper plot shows the absorption lines in each spectrum with the same transmission scale. Lower plots show the % calculated – observed residuals in an expanded vertical scale.

speaking, none of these two opposite models is adapted to the case of pure CO, since the perturbing molecule has the same mass as the radiative one. However, as observed in many other works (see, *e.g.* [21–23]), no significant difference was found between the collisional narrowing coefficients obtained by the two methods. We chose the Rautian profile which is easier to compute than the Galatry one [22,23]. Figure 3 shows that the “W” signatures are noticeably reduced when using the Rautian profile; however, a feature (neither symmetric nor anti-symmetric), larger than the noise level, remains in the residuals: this is probably due to the difficulty to treat a so weak effect and to the fact that the theoretical profile used to calculate the absorption coefficient is not perfectly adapted.

When trying to determine the collisional narrowing coefficient with the aid of the multispectrum procedure, we found that it was preferable to choose a Rautian profile only for the absorption coefficient of the three medium pressure spectra, for which the collisional narrowing is the most important, rather than for all the spectra. In this last case, the line parameters are slightly made worse, since an inadapted profile has been chosen for some spectra. (To be rigorous, one should also take into account the absorber speed dependence of the pressure broadening for the high pressure spectra, *e.g.* through a weighted sum of Lorentzian profiles [21]; however, this weak additional effect, not revealed by prominent anomalous signatures

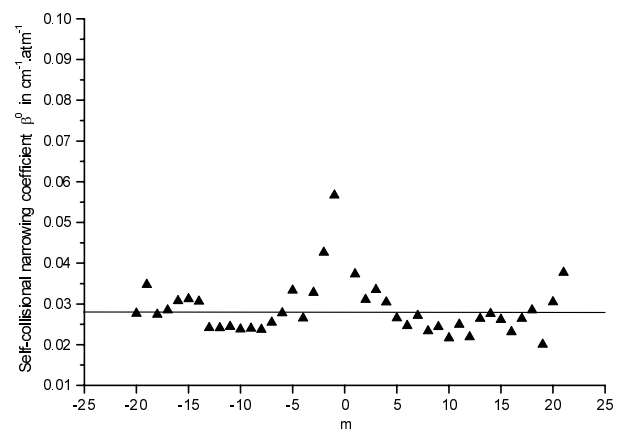


**Fig. 4.** Self-collisional narrowing coefficients of lines in the 3-0 band of  $^{12}\text{C}^{16}\text{O}$  vs.  $m$ , at about 296 K. The horizontal straight line indicates the average value used in this work.

in our fits, was neglected to avoid unnecessary complication of the treatment.) The collisional narrowing coefficient (Eqs. (10, 16)) is an example of parameter not easily determinable from a single spectrum when the effect is very weak (as in our CO spectra), and it is an advantage of the multispectrum method, already pointed out by Benner *et al.* [2], to allow the determination of such parameters. Figure 4 gives the obtained collisional narrowing coefficients  $\beta_0$  vs.  $m$ , with  $m = -J$  in the  $P$ -branch, and  $J+1$  in the  $R$ -branch,  $J$  being the rotational quantum number of the lower level of the transition. Theoretically, one should not observe a rotational dependence, at first order, for  $\beta_0$  [23–25]. The increasing of  $\beta_0$  for low  $J$  lines is perhaps an artifact of computation, due to the difficulty to retrieve  $\beta_0$  for lines having large broadening coefficient, the two parameters  $\beta_0$  and  $\gamma_0$  being strongly correlated [23–25]. However, such a striking effect was already observed by Pine and Looney for other molecules [24], suggesting that velocity changing collisions could be more probable for slowly rotating molecules [24]. Finally, we thought more advisable to calculate an average value: one finds  $\beta_0 = 0.028 \pm 0.004\text{ cm}^{-1}\text{ atm}^{-1}$  (1 atm = 1013 hPa) at about 296 K. At our knowledge, such a result has never been published, so that one can only compare with the value  $0.025\text{ cm}^{-1}\text{ atm}^{-1}$ , deduced from the self-diffusion mass coefficient  $0.187\text{ cm}^2\text{ s}^{-1}$  at 1 atm and 296 K, that we calculated using the data of [26]. The agreement is very satisfactory. In the final run of the multispectrum procedure, we fixed  $\beta_0$  at  $0.028\text{ cm}^{-1}\text{ atm}^{-1}$  to calculate the absorption coefficient in the three concerned spectra.

### 3.2.2 New line parameters for the 3-0 band of $^{12}\text{C}^{16}\text{O}$

The slightly improved line intensities and self-broadening coefficients obtained are given in Tables 2 and 3. Even if the improvements in the obtained line parameters are not quantitatively important, we thought useful to calculate new values for the vibrational dipole moment squared

$|\mu_0|^2$  and Herman-Wallis coefficients. Using the same formalism as in [6] for the dipole moment squared  $|\mu|^2$ :

$$|\mu|^2 = |\mu_0|^2 (1 + Cm + Dm^2), \quad (1)$$

we found:  $|\mu_0|^2 = (1.6730 \pm 0.0012) \times 10^{-7}$  Debye<sup>2</sup> (1 Debye =  $3.33546 \times 10^{-30}$  C m),  $C = (1.1996 \pm 0.0039) \times 10^{-2}$ , and  $D = (1.2498 \pm 0.0036) \times 10^{-4}$ , the quoted uncertainties being 68% confidence intervals (one standard deviation). These values are in very good agreement with those obtained in [6] and with those recently published by Henningsen *et al.* [20], confirming that the 6% absolute uncertainty stated in [6] is probably pessimistic [20]. Then, the 1996 HITRAN values [17], converted to pure <sup>12</sup>C<sup>16</sup>O at 296 K, can definitely be considered as too high by about 7.5%. Finally, Table 2 shows the good quality of the results, considering the very small observed – calculated differences we obtained.

In the same goal, we reduced the self-broadening coefficients  $\gamma_0$  adjusting their measured values by an empirical polynomial expansion *vs.*  $|m|$ :

$$\gamma_0 = A + \sum_{n=1}^{n=4} B_n |m|^n \quad (2)$$

with, in  $\text{cm}^{-1} \text{atm}^{-1}$  at 296 K:  $A = (9.392 \pm 0.036) \times 10^{-2}$ ,  $B_1 = (-6.86 \pm 0.22) \times 10^{-3}$ ,  $B_2 = (6.45 \pm 0.40) \times 10^{-4}$ ,  $B_3 = (-2.98 \pm 0.27) \times 10^{-5}$ , and  $B_4 = (4.94 \pm 0.62) \times 10^{-7}$ . This polynomial reproduces well the observed data inside the range of involved  $m$  values (see Tab. 2). For  $|m|$  greater than 20, we recommend to fix the self-broadening coefficient at a constant mean value of about  $54 \text{ cm}^{-1} \text{atm}^{-1}$ . One should also note that our measured self-broadening coefficients are in very good agreement with the HITRAN values [17].

### 3.3 Advantages of the multispectrum method

First of all, the method appears considerably time saving. We have also seen that it allowed to obtain a parameter (the collisional narrowing) not easily determinable from a single spectrum. But other advantages were found and are discussed below.

#### 3.3.1 Improvement of the statistical uncertainty of the results

The precision given by the confidence intervals of the obtained parameters is slightly decreased compared with the spectrum-by-spectrum method, as pointed out and discussed by Plateaux *et al.* [3]. However, this effect is not quantitatively so much important (see Tabs. 2 and 3). Furthermore, only statistical uncertainties are taken into account, but not possible systematic errors (see detailed discussion in [6]) present in all the spectra. To improve the accuracy (in other words, the uncertainty in the absolute values), one should treat simultaneously a very large

number of spectra, recorded with numerous different instruments, and under various experimental conditions. In such an ideal case, possible systematic errors present only in some classes of spectra would be taken into account, and the confidence intervals would “tend” to well estimate the absolute uncertainty; however, such a situation is not common, even if the method is able to treat spectra becoming from different spectrometers.

#### 3.3.2 Stability of the results obtained from the multispectrum method with respect to its utilization conditions

The multispectrum method leads to very stable values of the adjusted parameters, independently on the conditions of the study, inside reasonable limits, but even for conditions relatively far from those that would be chosen to match the absorption conditions of each spectrum. Table 4 gives the results obtained for the  $P1$  line using very different sets of “adjusted” spectral domains. Particularly, wide domains (up to  $2 \text{ cm}^{-1}$ ) were chosen in low pressure spectra where the line is not very pressure-broadened. One sees that the dispersion of the results is only about 0.6%. This is mainly due to the good quality of the spectra of a simple molecule as CO, but several tests led to a similar conclusion with more complicated molecular spectra.

Numerous tests were performed, changing the set of spectra chosen to be treated simultaneously. We have selected the most interesting of these tests in Table 5, and the conclusion is that the values obtained for a given parameter are not sensitive to the chosen spectra, provided that at least one spectrum, bringing a significant information on the concerned parameter, is taken into account. Let us examine in more details the results of Table 5.

As with the spectrum-by-spectrum method, it is not possible to obtain a parameter if one does not take into account the spectra containing information on this parameter. For example, if one eliminates the pressure-broadened spectra 4-7, which contain information on the collisional widths, the multispectrum method does not lead to a significant self-broadening coefficient, and consequently, the derived line intensity is damaged (see test 1 of Tab. 5). However, if one takes into account, in addition, at least one of the spectra previously omitted (see tests 2 and 3), the new information now available is enough to lead to a significant self-broadening coefficient, whose value is very close to the value obtained when all the spectra are taken into account. Moreover, as expected, the addition of one spectrum in the set of treated spectra significantly reduces the statistical uncertainty.

Conversely, let us suppose one takes into account only a few spectra (for example, two spectra) among the available spectra. Two interesting cases occur:

- a. these two spectra have been recorded under similar experimental conditions, bringing information both on intensities and collisional widths: for example, high pressure spectra 6 and 7. In this case, the obtained line parameters do not differ from each other by more than 1% (see test 4);

**Table 4.** Effect of the chosen “adjusted” spectral domains on the obtained parameters for the  $P1$  line of the 3-0 band of  $^{12}\text{C}^{16}\text{O}$ <sup>a</sup>.

Spectrum #	“Adjusted” spectral domains ( $10^{-3} \text{ cm}^{-1}$ )				
1	100	200	400	1000	2000
2	100	200	400	1000	2000
3	100	200	400	1000	2000
4	200	300	600	1000	2000
5	300	400	1000	1000	2000
6	600	600	1500	1000	2000
7	1000	1000	2000	1000	2000
$k_{\sigma}^N(T_0)$ ( $10^{-24} \text{ cm molecule}^{-1}$ )	3.9676(98)	3.9927(76)	4.0037(63)	4.022(72)	4.0146(64)
$\gamma_{(\text{self})}^0(T_0)$ ( $10^{-3} \text{ cm}^{-1} \text{ atm}^{-1}$ )	87.46(25)	87.95(23)	88.33(21)	88.59(23)	88.60(23)

<sup>a</sup>The statistical uncertainties of our results, between parenthesis, are 68% confidence intervals (one standard deviation in units of the last digit). Our results have been reported with all digits significant with respect to the quoted statistical uncertainties, in order to well exhibit the stability of the results; however, only at most three digits are actually significant according to the estimated accuracies.  $T_0$  is the standard temperature (296 K).

**Table 5.** Parameters obtained for the  $P1$  line of the 3-0 band of  $^{12}\text{C}^{16}\text{O}$ , from various sets of spectra chosen to be treated simultaneously by the multispectrum method<sup>a</sup>.

Test #	Used spectra	$k_{\sigma}^N(T_0)$ ( $10^{-24} \text{ cm molecule}^{-1}$ )	$x$ %	$\gamma_{(\text{self})}^0(T_0)$ ( $10^{-3} \text{ cm}^{-1} \text{ atm}^{-1}$ )	$x$ %
0	1, 2, 3, 4, 5, 6, 7	3.9837(67)	–	87.89(21)	–
1	1, 2, 3	4.038 (17)	1.4	98.0 (51)	11.5
2	1, 2, 3, 7	3.9670(68)	–0.4	87.39(18)	–0.6
3	1, 2, 3, 6, 7	3.9738(64)	–0.2	87.55(16)	–0.4
4	6, 7	3.9525(80)	–0.8	87.12(19)	–0.9
5	1, 7	3.9480(80)	–0.9	87.01(20)	–1.0

<sup>a</sup>See footnote of Table 4.  $x$  is, in percentage, the ratio between the value of the line parameter (intensity or self-broadening coefficient) obtained for the corresponding test, and the reference value obtained by the multispectrum method (test 0).

b. these two spectra correspond to “opposite” experimental conditions: for example, low pressure spectrum 1 (information on intensities only) and high pressure spectrum 7 (information both on intensities and collisional widths). In this case, again, one sees that the obtained line parameters do not differ from each other by more than 1% (see test 5).

One can notice the efficiency of the multispectrum method in test 5, which would have been particularly difficult to treat by the spectrum-by-spectrum method (many “manual” iterations required: at first, to fix the collisional widths for spectrum 1 to the values found with spectrum 7, then to fix the line intensities for spectrum 7 to the values thus obtained with spectrum 1, in order to obtain improved collisional widths, and so on up to convergence to sufficiently stable couples of values for line intensities and collisional widths). Finally, the multispectrum method present numerous advantages when one has at its disposal only a reduced sample of experimental spectra, whose absorption conditions are not entirely optimal.

### 3.3.3 Effects of systematic errors

As seen previously (Sect. 3.2.1) in the case of the collisional narrowing, systematic errors can occur if the expression of the absorption coefficient used in the calculation is inadequate. Also, Benner *et al.* [2] showed that the multispectrum method led to anomalously large residuals for spectra exhibiting a line mixing, when this one is not taken into account in the calculation.

In this work, we tested the multispectrum method by simulating several kinds of experimental errors in some of the treated spectra, and comparing the results with those obtained from the spectrum-by-spectrum method. For example, let us simulate an error in the absorbing gas amount of spectrum 6, that one has chosen because it brings important information both on line intensities and collisional widths (we chose a non-realistic 10% large error to better exhibit the effect). Figure 5 shows that this error in the pressure induces an anomalous symmetric signature in the residuals of the concerned spectrum. In the spectrum-by-spectrum method, such a signature could

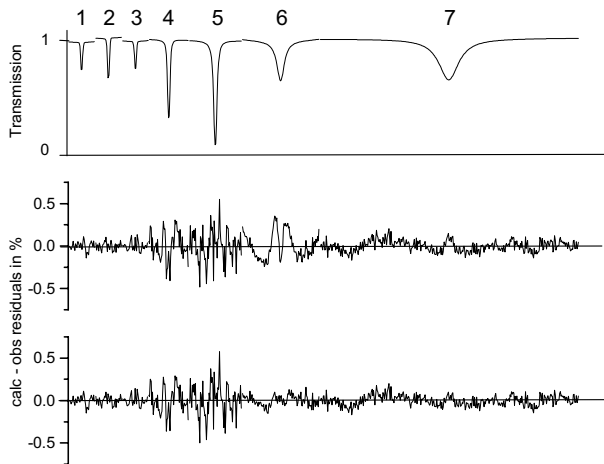


**Fig. 5.** Multispectrum adjustment of the 3-0  $P1$  line of  $^{12}\text{C}^{16}\text{O}$  at  $6346.594\text{ cm}^{-1}$ , when an error has been simulated in the pressure of one of the spectra (10% in the pressure of spectrum 6). The first row of residuals corresponds to the multispectrum fit with the erroneous pressure; and the second row corresponds to the multispectrum fit with the right pressure. (See caption of Fig. 3 for the general disposition of the plot.)

not be observed since the spectra are separately treated, so that the error could only be suspected when comparing the results obtained from each spectrum. Another advantage of the multispectrum method is shown in Table 6: even if not corrected, the error in the pressure leads to systematic errors in line parameters smaller for the multispectrum method than for the spectrum-by-spectrum one. In fact, this can be generalized to any type of systematic error occurring in only a few spectra: one can check that the consequences of such an error are always more important for the spectrum-by-spectrum method than for the multispectrum one.

### 3.3.4 Difficulties encountered in the determination of line positions and pressure-shifts. Calibration of the wavenumber scale

Accurate line positions and pressure-shifts (Eqs. (12, 13)) are much more difficult to determine than line intensities and collisional widths, taking into account the high accuracy attainable for the wavenumbers.

Even when the wavenumber scale of the spectra cannot be calibrated (for example, because the spectra do not contain lines belonging to a molecule whose line positions are known standard wavenumbers), it remains always possible to use the spectrum-by-spectrum method, knowing that one will not be able to deduce absolute zero pressure line positions nor pressure-shifts. In the same conditions, the multispectrum method defects. Indeed, in the “general” multispectrum option (see Sect. 2), the zero pressure line positions and the pressure-shifting coefficients are free parameters that have to keep the same values in all the spectra. When applied, the “general” multispectrum option exhibits characteristic antisymmetric signatures in the residuals (see Fig. 6), revealing that the

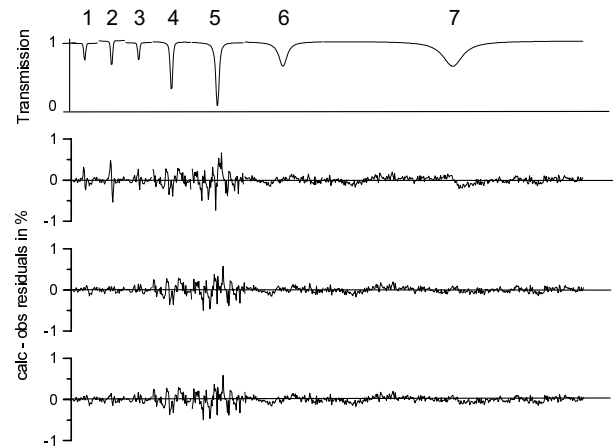


**Fig. 6.** Multispectrum adjustment of the 3-0  $P1$  line of  $^{12}\text{C}^{16}\text{O}$  at  $6346.594\text{ cm}^{-1}$ . The residuals correspond to the following cases: first row of residuals, in the absence of calibration of the wavenumber scales and using the “general” multispectrum option; second row, in the absence of calibration of the wavenumber scales but using the “reduced” multispectrum option; third row, the wavenumber scales being calibrated with respect to  $\text{C}_2\text{H}_2$  lines, and using the “general” multispectrum option. (See caption of Fig. 3 for the general disposition of the plot.)

relative wavenumber calibration is not perfect and that the obtained line positions and shifts are erroneous; consequently, other derived line parameters could also be perturbed. That is why we set up a “reduced” multispectrum option, in which the line positions (now pressure-shifted) are liable to be let free in each spectrum. In these conditions, it is no longer possible to adjust absolute zero pressure wavenumbers nor pressure-shifting coefficients, but one still benefits of the advantages of the multispectrum procedure when determining other line parameters as intensities or pressure-broadening coefficients. Also, Figure 6 shows that the signatures disappear in this case.

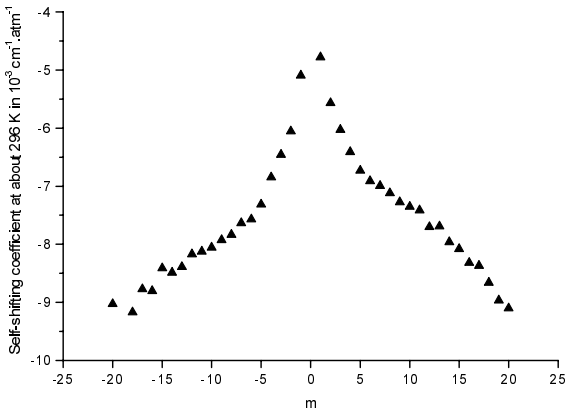
The spectra used in this work had not been especially recorded to deduce absolute positions and pressure-shifts. Nevertheless, as 6 torr of acetylene were put in a second cell crossed by the beam, an absolute calibration can be attempted by using  $\text{C}_2\text{H}_2$  standard line positions around  $6500\text{ cm}^{-1}$  measured by Kou *et al.* [27]. The line positions of [27] had to be slightly corrected with respect to more accurate data obtained by Nakagawa *et al.* [28] (we could not measure the  $\text{C}_2\text{H}_2$  lines of [28] because they were saturated in our spectra, their tops being used to check the linearity of the signal, which is important to retrieve accurate line intensities and widths). The self-shifting coefficient of acetylene [29] has been taken into account in the calibration, leading to a very small correction of  $-4 \times 10^{-5}\text{ cm}^{-1}$  at 6 torr. Then, one can try the “general” multispectrum option. The self-pressure shifting coefficients thus obtained have been plotted in Figure 7.

It is interesting to compare the self-shifting coefficients obtained by the “general” multispectrum method with those one can deduce from the pressure-shifted line positions obtained by the “reduced” multispectrum

**Table 6.** Parameters obtained for the *P*1 line of the 3-0 band of  $^{12}\text{C}^{16}\text{O}$ , when an error exists in the pressure of one of the spectra treated simultaneously<sup>a</sup>.

	(1) SBS Spectrum 6 right pressure	(2) SBS Spectrum 6 erroneous pressure	(3) ⟨SBS⟩ With spectrum 6 right pressure	(4) ⟨SBS⟩ With spectrum 6 erroneous pressure	(4)/(3) %
$k_{\sigma}^N(T_0)$ ( $10^{-24}$ cm molecule $^{-1}$ )	4.020(19)	4.465(21)	$4.019 \pm 0.023$	$4.08 \pm 0.06$	1.5
$\gamma_{(\text{self})}^0(T_0)$ ( $10^{-3}$ cm $^{-1}$ atm $^{-1}$ )	88.49(42)	98.25(47)	$89.2 \pm 1.4$	$92.5 \pm 2.7$	3.7
			(5) MSF With spectrum 6 right pressure	(6) MSF With spectrum 6 erroneous pressure	(6)/(5) %
$k_{\sigma}^N(T_0)$ ( $10^{-24}$ cm molecule $^{-1}$ )			3.9837(67)	4.0086(79)	0.6
$\gamma_{(\text{self})}^0(T_0)$ ( $10^{-3}$ cm $^{-1}$ atm $^{-1}$ )			87.89(21)	88.67(25)	0.9

<sup>a</sup> See footnote of Table 4. Columns (1–4): line parameters obtained by the spectrum-by-spectrum method (SBS). Column (1): from spectrum 6 only with the right pressure. Column (2): from spectrum: 6 only with an erroneous pressure (–10%). Columns (3) and (4): averages of the results, obtained from the seven spectra for the intensities, and from spectra 4–6 for the self-broadening coefficients (the quoted statistical uncertainties are the standard deviations of the mean divided by  $\sqrt{7}$  for the line intensities, and by  $\sqrt{3}$  for the self-broadening coefficients, according to the number of spectra taken into account); column (3): with the value of column (1); and column (4): with the value of column (2). Columns (5) and (6): line parameters obtained by the multispectrum method (MSF); column (5): with the right pressure for spectrum 6; and column (6): with an erroneous pressure for spectrum 6.

**Fig. 7.** Self-shifting coefficients of lines in the 3-0 band of  $^{12}\text{C}^{16}\text{O}$  vs.  $m$ , at about 296 K. Note that the values obtained for the *P*19 and *R*20 lines could not be retained because of the presence of very weak lines due to traces of  $\text{CO}_2$  inside the evacuated tank of the interferometer. (The best values of self-shifting coefficients currently available can be found in [30].)

vs. pressure. One can see that the pressure-shift is proportional to the pressure, as expected. The straight line plotted in Figure 8 is the result of a linear adjustment of the data, and its slope gives the self-shifting coefficient of the concerned line. To make a consistent comparison with the self-shifting coefficient obtained by the “general” method ( $-8.21 \times 10^{-3}$  cm $^{-1}$  atm $^{-1}$ ), one has to take into account the standard deviation of each line position obtained by the “reduced” method. Thus, the straight line in Figure 8 has been obtained through a linear least-squares fit, the data being weighted according to the reciprocal of their standard deviation squared. One finds  $-8.18 \times 10^{-3}$  cm $^{-1}$  atm $^{-1}$ , in very good agreement with the value obtained by the “general” multispectrum method. The zero pressure line positions are also in good agreement:  $6\,297.410\,057$  cm $^{-1}$  for the “general” method, and  $6\,297.410\,060$  cm $^{-1}$  for the “reduced” one. This shows the coherence of the two methods.

## 4 Conclusion

method (the wavenumber scales being calibrated). For that, the *P*12 line has been chosen as example: Figure 8 is a plot of the *P*12 pressure-shifted line positions

In this work, a multispectrum fitting procedure was set up in order to obtain line parameters, at once from several spectra. This method has been tested with the aid of

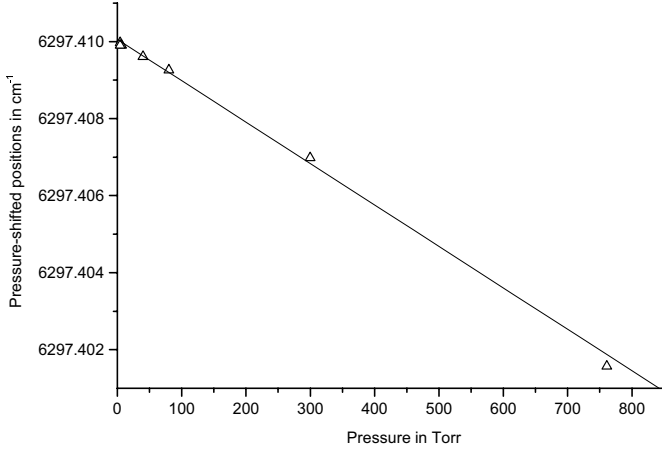


**Fig. 8.** Pressure-shifted positions of the 3-0  $P_{12}$  line of  $^{12}\text{C}^{16}\text{O}$ , at  $6297.410\text{ cm}^{-1}$ , *vs.* pressure, obtained from the “reduced” multispectrum method, the wavenumber scales being calibrated.

Fourier transform absorption spectra of the 3-0 band of CO. The obtained line intensities and self-broadening coefficients have been found in very good agreement with previously published results, and could be slightly improved taking into account the self-collisional narrowing observed for the first time on Fourier transform CO spectra. The advantages of the method have been pointed out and illustrated with typical examples. Even when the calibration of the wavenumber scale cannot be achieved with high accuracy, the method can still be used letting free the pressure-shifted line positions in each spectrum. Coherent CO self-shifting coefficients have been deduced and compared with previous results.

To conclude, let us summarize the advantages that we found in the multispectrum method, *vs.* the spectrum-by-spectrum one:

1. this method is noticeably time-saving;
2. this method is versatile: the values deduced for the line parameters remain stable with respect to the utilization conditions of the method (inside realistic changes of these conditions);
3. the precision (statistical uncertainty) of the line parameters is slightly improved;
4. some systematic errors, present in one of the treated spectra, can be detected through anomalous signatures in the observed – calculated residuals of the fit of this spectrum;
5. the values deduced for the line parameters are less sensitive to possible systematic errors present in some spectra, improving the accuracy (absolute uncertainty) of the results;
6. the method is able to retrieve some parameters that cannot easily be determined from a single spectrum.

In a near future, we will study line parameters in numerous overlapping bands of acetylene in the  $5\ \mu\text{m}$ -region. This will be an opportunity to test again the behavior of the multispectrum procedure, by extensively applying it to crowded and rather complicated spectra.

## Appendix A: Basic relationships, physics, and definitions

### A.1 Equations used to calculate the transmission in absorption molecular gas spectra

We give below the string of the main equations that have to be encoded to calculate the transmission:

$$\tau_{\text{calc}_s}(\sigma_{is}) = \int_0^{+\infty} \{ \tau_s(\sigma) \times [A_{cs} + B_{cs}(\sigma - \sigma_c) + C_{cs}(\sigma - \sigma_c)^2] \} \times f_{\Phi_{cs}, (R_{cs}/F_s)^2}(\sigma - \sigma_{is}) d\sigma, \quad (3)$$

$$\tau_s(\sigma) = \exp[-L_s K_s(\sigma)], \quad (4)$$

$$K_s(\sigma) = \sum_{n_s} K_{n_s}(\sigma) \quad (5)$$

$$K_{n_s}(\sigma) = k_{\sigma n}^P(T_s) P_s^{(a)} \frac{1}{\gamma_{cs}^D} \left( \frac{\ln 2}{\pi} \right)^{1/2} \times k_s(x_{n_s}(\sigma), y_{n_s}, z_{n_s}) \quad (6)$$

$$k_{\sigma n}^P(T_s) = L_0 \frac{273.15}{T_s} k_{\sigma n}^N(T_0) \times \frac{Z(T_0)}{Z(T_s)} \exp \left[ \frac{hcE_n''}{k_B} \left( \frac{1}{T_0} - \frac{1}{T_s} \right) \right] \quad (7)$$

$$\gamma_{cs}^D \approx 3.58 \times 10^{-7} \left( \frac{T_s}{M} \right)^{1/2} \sigma_c \quad (8)$$

$$x_{n_s}(\sigma) = (\ln 2)^{1/2} \frac{\sigma - \sigma_{n_s}^0}{\gamma_{cs}^D} \quad (9)$$

$$y_{n_s} = (\ln 2)^{1/2} \frac{\gamma_{n_s}^L}{\gamma_{cs}^D} \quad (10)$$

$$z_{n_s} = (\ln 2)^{1/2} \frac{\beta_{n_s}}{\gamma_{cs}^D} \quad (11)$$

$$\sigma_{n_s}^0 = \sigma_n^0 + \delta_{n_s} \quad (12)$$

$$\delta_{n_s} = \delta_{(\text{self})_n}^0 P_s^{(a)} + \delta_{(1)_n}^0 P_s^{(1)} + \delta_{(2)_n}^0 P_s^{(2)} \quad (13)$$

$$\gamma_{n_s}^L = \gamma_{(\text{self})_{n_s}}^0(T_s) P_s^{(a)} + \gamma_{(1)_{n_s}}^0(T_s) P_s^{(1)} + \gamma_{(2)_{n_s}}^0(T_s) P_s^{(2)} \quad (14)$$

$$\gamma_{(G)_{n_s}}^0(T_s) = \gamma_{(G)_n}^0(T_0) (T_0/T_s)^{m_{(G)_n}} \quad (15)$$

$(G) = (\text{self}), (1), \text{ or } (2)$

$$\beta_{n_s} \approx \beta_n^0 (P_s^{(a)} + P_s^{(1)} + P_s^{(2)}). \quad (16)$$

### A.2 Nomenclature

We give below the meaning of the notations and of the physical quantities involved in the above equations. In these expressions:

- the subscript  $i$  refers to an experimental point of a given spectrum,
- the subscript  $s$  refers to a given spectrum,

- the subscript  $n$  refers to a given line to take into account,
- the subscript  $c$  refers to the line under study,
- the superscript (a) and the subscript (self) refer to the absorbing gas (strictly speaking, the studied absorbing isotopic species),
- the superscripts or subscripts (1) and (2) refer to possible other gases present in the cell,
- $\tau_{\text{calc}_s}$  is the calculated whole transmission in spectrum  $s$ ,
- $\sigma_{is}$  is the wavenumber of an experimental point  $i$  belonging to spectrum  $s$ ,
- $\tau_s$  is the calculated whole transmission in spectrum  $s$ , under infinite resolution,
- $A_{cs}$ ,  $B_{cs}$ , and  $C_{cs}$  are the coefficients of a polynomial representation of the continuous background in spectrum  $s$ , and around the line under study, located at the center  $\sigma_c$  of the “adjusted” spectral domains,
- $f_{\Phi_{cs}}^{(s)}, (R_{cs}/F_s)^2$  is the apparatus function adapted to spectrum  $s$ ,
- $\Phi_{cs}$  is the phase error (in radian) in spectrum  $s$ , and around the wavenumber  $\sigma_c$ ,
- $R_{cs}$  is the effective iris radius, in spectrum  $s$ , determined when treating line  $c$ ,
- $F_s$  is the collimator focal length, in spectrum  $s$ ,
- $L_s$  is the absorbing path length, in spectrum  $s$ ,
- $K_s$  is the whole absorption coefficient, in spectrum  $s$ ,
- $K_{n_s}$  is the absorption coefficient due to line  $n$ , in spectrum  $s$ ,
- $k_{\sigma n}^P$  is the integrated absorption coefficient at unit pressure (in  $\text{cm}^{-2} \text{atm}^{-1}$ ) of line  $n$ ,
- $P_s$  is a partial pressure, for spectrum  $s$ ,
- $\gamma_{cs}^D$  is the Gaussian half-width due to Doppler broadening, in spectrum  $s$ , for the lines taken into account,
- $k_s$  is a reduced normalized profile function chosen for spectrum  $s$  (if the Voigt profile has been chosen, the reduced variable  $z$  is identical to zero),
- $L_0$  is Loschmidt’s number =  $2.686\,76 \times 10^{19}$  molecules  $\text{cm}^{-3} \text{atm}^{-1}$ ,
- $T_s$  is the temperature in the cell, for spectrum  $s$ ,
- $M$  is the molar mass (in g) of the absorbing molecule,
- $k_{\sigma n}^N(T_0)$  is the line intensity (in  $\text{cm mol}^{-1}$ ) at the standard temperature  $T_0 = 296$  K, of line  $n$ ,
- $Z$  is the total partition function of the absorbing molecule,
- $hcE_n''$  is the energy (in  $\text{cm}^{-1}$ ) of the lower level of the transition corresponding to line  $n$ ,
- $k_B$  is Boltzmann’s constant =  $1.380\,658 \times 10^{-16}$  erg  $\text{K}^{-1}$  (1 erg =  $10^{-7}$  J),
- $\sigma_{n_s}^0$  is the position of line  $n$ , in spectrum  $s$ ,
- $\sigma_n^0$  is the position of line  $n$  at zero pressure,
- $\delta_{n_s}$  is the pressure-shift of line  $n$ , in spectrum  $s$ ,
- $\delta_{(G)_n}^0$  is a pressure-shifting coefficient of line  $n$ ,
- $\gamma_{n_s}^L$  is the Lorentzian half-width due to collisional broadening, for line  $n$ , in spectrum  $s$ ,
- $\gamma_{(G)_n}^0(T_0)$  is a pressure-broadening coefficient of line  $n$ , at the standard temperature  $T_0 = 296$  K,
- $m_{(G)_n}$  is the temperature dependence exponent of a pressure-broadening coefficient of line  $n$ ,

- $\beta_{n_s}$  is the collisional narrowing parameter of line  $n$ , in spectrum  $s$ ,
- $\beta_n^0$  is the collisional narrowing coefficient of line  $n$ .

### A.3 Physical meaning of the equations

We recall briefly the physical meaning of the equations quoted in this Appendix.

Equation (3) is the convolution product of the apparatus function with the transmission under infinite resolution, weighted by the local continuous background modeled by a parabola. The apparatus function of the interferometer [8–10] depends upon the following adjustable parameters: the “*étendue*” (through the ratio of the iris radius and the collimator focal length), and a possible phase error. (Note that it depends also upon the maximum path difference, which is a well known fixed quantity [8–10].)

Equation (4) is the Beer-Lambert law valid if the absorption cell is an homogeneous medium.

Equation (5) gives the whole absorption coefficient by adding the individual absorption coefficients of the overlapping lines. Such a summation is valid in the absence of line mixing, which is the case for the well isolated CO lines and the relatively low pressures considered in this work.

Equation (6) expresses the absorption coefficient *vs.* dimensionless variables, through a reduced normalized profile valid under the impact approximation: the Voigt profile [11] in the general case, and the Rautian or Galatry profiles [12–16] in case of collisional narrowing.

Equation (7) is the relationship between the line intensity at a standard temperature and the integrated absorption coefficient at unit pressure, for given temperature and transition.

Equation (8) defines the half-width at half-maximum of the reduced Gaussian absorption coefficient due to Doppler broadening.

Equations (9–11) define the dimensionless variables used in the reduced profile of equation (6).

Equation (12) expresses the pressure-shifted line position as the sum of a zero pressure line position and a pressure-shift.

Equations (13, 14) express the pressure-shift and the collisional width as a sum of pressure-shifts or collisional widths, respectively, each of them being due to one of the molecular species present in the cell. This is valid as far as only binary collisions occur, which is the case in our pressure conditions. In the same conditions, each contributing pressure-shift or collisional width is proportional to the partial pressure of the concerned buffer gas.

Equation (15) is the model commonly used to take into account the temperature dependence of the pressure-broadening coefficients. In the present work, the temperature dependence exponent could not be considered as a free line parameter, the temperatures of the studied spectra being too close to each other. Note that, at the present time, we have not yet introduced a temperature dependence for the pressure-shifts.

Equation (16) is the expression used in this work to calculate the collisional narrowing as proportional to the total pressure in the cell. This is an approximation valid for a pure gas in natural abundances. Note that, as for pressure-shifts and collisional widths, it would be easy to introduce several specific coefficients, each of them concerning a peculiar buffer gas. Furthermore, we have not introduced a temperature dependence for the collisional narrowing coefficients.

#### A.4 Free or fixed parameters

The free or fixed parameters of the least-squares method are the following.

The line parameters, *i.e.*, zero-pressure positions, intensities, pressure-broadening coefficients, pressure-shifting coefficients, and collisional-narrowing coefficients. In the “general” multispectrum option, they do not depend upon the spectrum; in the “reduced” multispectrum option, the line positions depend upon the spectrum and the pressure-shifting coefficients are not determined.

Some parameters related to the local continuous background:  $A_{cs}$ ,  $B_{cs}$ , and  $C_{cs}$ ; they depend upon the spectrum and the studied line.

Some parameters related to the apparatus function:  $\Phi_{cs}$  and  $R_{cs}$ ; their adjusted values depend upon the spectrum and the studied line. In the final run, these last parameters can be fixed to average values obtained from previous runs.

#### A.5 Glossary

The definitions of the main terms used in this paper are gathered below.

The “*spectrum-by-spectrum*” (*SBS*) *procedure* (or *method*, or *fitting*), is the usual least-squares fitting method in which each spectrum is treated separately, the parameters that are looked for being the averages of the values obtained for these parameters from each spectrum. In this method, no correlation is introduced between the spectra.

A “*multispectrum*” *procedure*, or *method*, or *fitting* (*MSF*), is a least-squares fitting method in which several spectra are treated simultaneously, and for which the parameters vector is not identical to the concatenation of the parameters vectors corresponding to each spectrum in the spectrum-by-spectrum procedure. In such a method, some correlations are introduced between the spectra, that is to say, there exists at least one free line parameter common to all the spectra.

In this paper, we call “*general*” *multispectrum procedure*, the particular case of multispectrum procedure for which all the free line parameters are common to all the spectra treated simultaneously (except for the collisional narrowing coefficient which is common to all the concerned spectra when it is let free).

In this paper, we call “*reduced*” *multispectrum procedure*, the particular case of multispectrum procedure for

which the free line parameters are common to all the spectra treated simultaneously (the collisional narrowing coefficient being fixed), except for the line positions that are let free in each spectrum, independently from each other.

In a given spectrum, the “*adjusted*” *spectral domain* is the spectral domain where the calculated transmission has to be adjusted to the experimental one.

In a given spectrum, the “*taken into account lines*” *spectral domain* is defined as follows: the transmission due to the lines centered inside this spectral domain, but outside the “adjusted” spectral domain, is taken into account with fixed line parameters in the calculation of the transmission inside the “adjusted” spectral domain.

In the “*automatic*” *version of a procedure*, the lines of one spectrum (in the case of the spectrum-by-spectrum method), or of several spectra (in the case of the multispectrum method), are treated sequentially and automatically, given some data as the “adjusted” and “taken into account lines” domains, and the list of free or fixed parameters.

In the “*manual*” *version of a procedure* (spectrum-by-spectrum or multispectrum), the overlapping lines of a chosen set are treated simultaneously, the operator being allowed to fix or let free any parameter, as well as to remove or to add some lines if necessary.

## References

1. M. Carlotti, Appl. Opt. **27**, 3250 (1988).
2. D.C. Benner, C.P. Rinsland, V. Malathy Devi, M.A.H. Smith, D. Atkins, J. Quant. Spectrosc. Radiat. Transfer **53**, 705 (1995).
3. J.-J. Plateaux, L. Régalia, C. Boussin, A. Barbe, J. Quant. Spectrosc. Radiat. Transfer **68**, 507 (2001).
4. V. Dana, J.-Y. Mandin, J. Quant. Spectrosc. Radiat. Transfer **48**, 725 (1992).
5. V. Dana, J.-Y. Mandin, C. Camy-Peyret, J.-M. Flaud, J.-P. Chevillard, R.P. Hawkins, J.-L. Delfau, Appl. Opt. **31**, 1928 (1992).
6. N. Picqué, G. Guelachvili, V. Dana, J.-Y. Mandin, J. Mol. Struct. **517-518**, 427 (2000).
7. M.L. Ralston, R.I. Jennrich, Technometrics **20**, 7 (1978).
8. J. Connes, Rev. Opt. Théor. Instrum. **40**, 45 (1961).
9. G. Guelachvili, in *Spectrometric Techniques*, edited by G.A. Vanasse (Academic Press, New York, 1981), Vol. II, pp. 1-62.
10. M.-Y. Allout, J.-Y. Mandin, V. Dana, N. Picqué, G. Guelachvili, J. Quant. Spectrosc. Radiat. Transfer **60**, 979 (1998).
11. W. Gautshi, Comm. ACM **12**, 635 (1969); W. Gautshi, SIAM J. Numer. Anal. **7**, 187 (1970); K.S. Kolbig, Comm. ACM **15**, 465 (1972).
12. R.H. Dicke, Phys. Rev. **89**, 472 (1953).
13. L. Galatry, Phys. Rev. **122**, 1218 (1961).
14. G. Millot, B. Lavorel, R. Saint-Loup, H. Berger, J. Physique (France) **46**, 1925 (1985).
15. P.L. Varghese, R.K. Hanson, Appl. Opt. **23**, 2376 (1984).
16. S.G. Rautian, I.I. Sobel'man, Sov. Phys. Uspekii **9**, 701 (1967).

17. L.S. Rothman, C.P. Rinsland, A. Goldman, S.T. Massie, D.P. Edwards, J.-M. Flaud, A. Perrin, C. Camy-Peyret, V. Dana, J.-Y. Mandin, J. Schroeder, A. McCann, R.R. Gamache, R.B. Wattson, K. Yoshino, K. Chance, K. Jucks, L.R. Brown, V. Nemtchinov, P. Varanasi, *J. Quant. Spectrosc. Radiat. Transfer* **60**, 665 (1998).
18. R.R. Gamache, R.L. Hawkins, L.S. Rothman, *J. Mol. Spectrosc.* **142**, 205 (1990).
19. R.R. Gamache, S. Kennedy, R. Hawkins, L.S. Rothman, *J. Mol. Struct.* **517-518**, 407 (2000).
20. J. Henningsen, H. Simonsen, T. Mogelberg, E. Trudso, *J. Mol. Spectrosc.* **193**, 354 (1999).
21. A. Henry, D. Hurtmans, M. Margottin-Maclou, A. Valentin, *J. Quant. Spectrosc. Radiat. Transfer* **56**, 647 (1996).
22. B.E. Grossmann, E.V. Browell, *J. Mol. Spectrosc.* **136**, 264 (1989).
23. M. Lepère, Thèse de doctorat en sciences, Facultés Universitaires Notre-Dame de la Paix, Namur, Belgium, 1999.
24. A.S. Pine, J.P. Looney, *J. Mol. Spectrosc.* **122**, 41 (1987).
25. A.S. Pine, J.P. Looney, *J. Chem. Phys.* **93**, 6942 (1990).
26. J.O. Hirschfelder, C.F. Curtiss, R.B. Bird, *Molecular Theory of Gases and Liquids* (Wiley, New York, 1964).
27. Q. Kou, G. Guelachvili, M. Abouti Tamsamani, M. Herman, *Can. J. Phys.* **72**, 1241 (1994).
28. K. Nakagawa, M. de Labachellerie, Y. Awaji, M. Kourogi, *J. Opt. Soc. Am. B* **13**, 2708 (1996).
29. Y. Sakai, S. Sudo, T. Ikegami, *IEEE J. Quantum Electron.* **28**, 75 (1992).
30. N. Picqué, G. Guelachvili, *J. Mol. Spectrosc.* **185**, 244 (1997).